

Charm production in association with an electroweak gauge boson at the LHC

W.J. Stirling, E. Vryonidou

Cavendish Laboratory, J.J. Thomson Avenue, Cambridge CB3 0HE, UK

The production of charm quark jets in association with electroweak gauge bosons at the LHC can be used as a tool to constrain quark parton distribution functions (PDFs). Motivated by recent measurements at the Tevatron and LHC, we calculate cross sections for $W/Z + c$, comparing these to $W/Z + \text{jet}$, for various PDF sets. The cross-section differences can be understood in terms of the different underlying PDFs, with the strange quark distribution being particularly important for $W + c$ production. We suggest measurements of appropriately defined ratios and comment on how these measurements at the LHC can be used to extract information on the strange and charm content of the proton at high Q^2 scales.

I. INTRODUCTION

The production of charm quarks in association with electroweak gauge bosons at hadron colliders can provide important information on strange and charm quark PDFs, complementary to that obtained by tagging charm quarks in the final state in deep inelastic scattering experiments [1]. In particular, the Tevatron CDF and D0 experiments [2, 3] have measured the cross section for charm quarks produced in association with W bosons, using muon tagging of the charm-quark jet. However the accuracy of these measurements is limited to $\sim 30\%$ by low statistics. The LHC is expected to provide a more precise measurement, and indeed the CMS collaboration has recently performed a similar study [4] of $W^\pm + c(\bar{c})$ production, again using muons to tag the charm quark jet in the final state.

At leading order (LO), the Feynman diagrams for charm production in association with a W boson are shown in Fig. 1. The dominant contribution comes from strange quark – gluon scattering, as the corresponding down-quark contribution is strongly Cabibbo suppressed. The cross section for $W + c$ production (where ‘ c ’ denotes

colliders, the strange and charm quarks are probed at much higher Q^2 ($\sim 10^4 \text{ GeV}^2$) values than in the traditional determinations from deep inelastic scattering, i.e. $\nu s \rightarrow \mu^- c(\rightarrow \mu^+)$ and $ec \rightarrow ec(\rightarrow \mu^+)$ where typically $Q^2 \sim 10^{0-2} \text{ GeV}^2$). Taken together, the measurements therefore also test DGLAP evolution for these quark flavours.

In this letter we study $W + c$ -jet production in the context of the CMS analysis [4], analysing the different quark contributions and comparing the predictions of various widely-used PDF sets. We also study the corresponding cross-section ratio for $Z + c$ -jet production, which should be measurable with the 2011 LHC data set.

II. CMS MEASUREMENT OF $\sigma(W + c)$

The two relevant cross-section ratios introduced by CMS [4] are:

$$R_c^\pm = \frac{\sigma(W^\pm + \bar{c})}{\sigma(W^\mp + c)} \quad \text{and} \quad R_c = \frac{\sigma(W + c)}{\sigma(W + \text{jet})}. \quad (1)$$

The advantage of using ratios is that many of the theoretical and experimental uncertainties cancel. In particular, the ratios are fairly insensitive to higher-order perturbative QCD corrections. Note that $R_c^\pm \equiv 1$ at the Tevatron. We calculate the cross sections at NLO pQCD using MCFM [5], applying the CMS cuts [4] to the final-state: $p_T^j > 20 \text{ GeV}$, $|\eta^j| < 2.1$, $p_T^l > 25 \text{ GeV}$, $|\eta^l| < 2.1$, $R = 0.5$, $R^{lj} = 0.3$. Five different NLO PDF sets are used: CT10 [6], MSTW2008 [7], NNPDF2.1 [8], GJR08 [9] and ABKM09 [10], as implemented in LHAPDF [11]. The renormalisation and factorisation scales are set to M_W , although the cross-section ratios are rather insensitive to this choice. (We have also considered dynamical scales of the form $Q^2 = M_W^2 + p_{TW}^2$, but the differences for the cross-section ratios are similar in magnitude to the PDF uncertainties.)

The results are summarised in Table I where we also include the ratio:

$$R^\pm = \frac{\sigma(W^\pm + \text{jet})}{\sigma(W^\mp + \text{jet})}. \quad (2)$$



FIG. 1: Feynman diagrams for $W^\pm + c(\bar{c})$ production at leading order.

a tagged charm-quark jet) is measured in Ref. [2] (CDF), while Ref. [3] (D0) introduces the ratio of charm jets to all jets, which is expected to suffer less from both experimental and theoretical uncertainties. CMS has performed a similar analysis [4] using the 2010 LHC data set.

Also of interest is charm production in association with Z bosons. The leading-order process is simply $cg \rightarrow Zc$, and so this process can be used to extract information on the charm quark PDF. It is important to note that for both $W + c$ and $Z + c$ production at hadron

Ratio	R_c^\pm	R_c	R^\pm
CT10	$0.953^{+0.009}_{-0.007}$	$0.124^{+0.021}_{-0.012}$	$1.39^{+0.03}_{+0.03}$
MSTW2008NLO	$0.921^{+0.022}_{-0.033}$	$0.116^{+0.002}_{-0.002}$	$1.34^{+0.01}_{-0.01}$
NNPDF2.1NLO	0.944 ± 0.008	0.104 ± 0.005	1.39 ± 0.02
GJR08	0.933 ± 0.003	0.099 ± 0.002	1.37 ± 0.02
ABKM09	0.933 ± 0.002	0.116 ± 0.003	1.39 ± 0.01

TABLE I: Comparison of results for the cross-section ratios defined in (1) and (2) at NLO using different PDF sets, including 68%cl (asymmetric, where available) PDF errors.

We note that our values for R_c^\pm are systematically larger by $\sim 3\%$ than those quoted in the CMS study [4], but we are unable to account for this difference. We have also checked that the values are stable with respect to NLO corrections, with the difference from the LO results being within 1% for R_c^\pm and 3% for R_c . In what follows we restrict our analysis to the three global PDF sets CT10, MSTW2008 and NNPDF2.1, since these span a relatively broad range of predictions for the cross section ratios.

For reference, we note that the values of R_c^\pm and R_c measured by CMS are:

$$R_c^\pm = 0.92 \pm 0.19 \text{ (stat.)} \pm 0.04 \text{ (syst.)} \quad (3)$$

$$R_c = 0.143 \pm 0.015 \text{ (stat.)} \pm 0.024 \text{ (syst.)} \quad (4)$$

Note that the experimental systematic errors are already of the same order as the differences between the predictions of the various PDF sets.

If the strange quark contribution to $W + c$ production were totally dominant, then any deviation of R_c^\pm from 1 would imply an asymmetry between s and \bar{s} . However even if $s = \bar{s}$, the fact that $\bar{d} < d$ will automatically give $R_c^\pm < 1$ through the Cabibbo suppressed d -quark contribution. Schematically, at LO we expect

$$R_c^\pm \sim \frac{\bar{s} + |V_{dc}|^2 \bar{d}}{s + |V_{dc}|^2 d}, \quad (5)$$

with $V_{dc}=0.225$. This leads to a suppression by a factor of 20 of the d -quark contribution.

The contributions (in fb) from d and s quarks to the LO $W + c$ cross sections are shown in Table II and the corresponding percentages in Table III. The cross-section values correspond to the leptonic decay channel $W \rightarrow e\nu$. These are obtained using LO subprocesses (but calculated with NLO PDFs) since the presence of additional NLO subprocesses does not permit a simple quark-flavour decomposition.

The relative contributions of initial-state s and d quarks to the $W + c$ cross-section ratios R_c^\pm and R_c are illustrated in Figs. 2 and 3. For CT10 $s = \bar{s}$ and therefore the fact that $R_c^\pm < 1$ is due entirely to the difference between d and \bar{d} in the Cabibbo suppressed $dq \rightarrow Wc$ subprocess. NNPDF2.1 does have an asymmetric strange

Process	CT10	MSTW2008NLO	NNPDF2.1NLO
$W^+ + \bar{c}: \bar{s}$	39934	37133	32980
$W^+ + \bar{c}: \bar{d}$	2666	2854	2880
$W^- + c: s$	39987	38449	33012
$W^- + c: d$	4969	5178	5180

TABLE II: Cross section contributions (in fb) of d -quarks to $\sigma(W + c) \cdot B(W \rightarrow e\nu)$ for different NLO PDFs at LO.

Process	CT10	MSTW2008NLO	NNPDF2.1NLO
$W^+ + \bar{c}$	6.3	7.1	8.0
$W^- + c$	11.1	11.9	13.6

TABLE III: Percentage contribution of d -quarks to $\sigma(W + c)$ for different NLO PDFs at LO.

sea, $s - \bar{s} \neq 0$, but the asymmetry turns out to be very small in the x, Q^2 region of interest for this process and therefore $R_c^\pm \neq 1$ is again determined mainly by the d, \bar{d} asymmetry. Finally, for MSTW2008 the strange asymmetry is larger and therefore contributes significantly to R_c^\pm . Here the (LO) ratio of $\sigma(W^+ + \bar{c})$ to $\sigma(W^- + c)$ obtained by setting d -quark PDFs to zero is ~ 0.96 , and this is decreased further by the asymmetry in d and \bar{d} .

The strange asymmetry $s - \bar{s}$ for $Q = M_W$, the relevant scale for this process, is shown in Fig. 4, including the 68%cl uncertainty band in the case of MSTW2008NLO and NNPDF2.1. The strange asymmetry in both of these sets is constrained by the CCFR and NuTeV dimuon νN and $\bar{\nu} N$ DIS data [12] in the global fit. These data slightly prefer an asymmetric strange sea in the x range $0.03 - 0.3$, although the CT10 symmetric choice of $s = \bar{s}$ is also consistent with the data within errors. In the MSTW2008NLO fit, the strange asymmetry is parameterised ‘minimally’ as

$$\begin{aligned} s_V(x, Q_0^2) &\equiv s(x, Q_0^2) - \bar{s}(x, Q_0^2) \\ &= A_- x^{\delta_- - 1} (1 - x)^{\eta_-} (1 - x/x_0), \end{aligned} \quad (6)$$

with the overall constraint that $\int_0^1 dx s_V(x, Q_0^2) = 0$. It is this choice of parametrisation that drives the relatively large positive asymmetry in the range $x \sim 0.01 - 0.1$. There is no such strong parameterisation dependence in the NNPDF2.1 fit. A precise measurement of the ratio R_c^\pm , combined with an improved knowledge of the d, \bar{d} difference (for example, from the rapidity dependence of the inclusive $W \rightarrow \ell\nu$ charge asymmetry), could therefore provide important new information on the strange sea asymmetry at small x .

The cross-section ratio R_c can be used as a measure of the *total* strangeness of the proton, and to the extent that these W -jet cross sections are dominated by qg scattering we can expect $R_c \sim \frac{s+\bar{s}}{\Sigma(q+\bar{q})}$. For our three sets of NLO PDFs this ratio at scale $Q = M_W$ is shown in Fig. 5. We note that the ordering of the R_c values

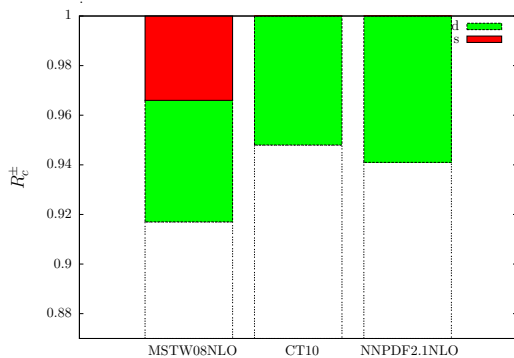


FIG. 2: Effect of initial-state s and d quarks on R_c^\pm using NLO PDFs and LO subprocesses.

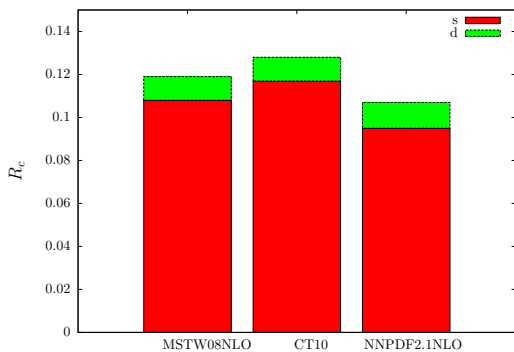


FIG. 3: Effect of s and d quarks on R_c using NLO PDFs (LO processes).

for the different PDF sets, see Table I, agrees qualitatively with the corresponding values of the quark ratio at $x \sim 0.06$, the average value of the incoming quark x for this collider energy and choice of cuts. We also see that the relative size of the PDF uncertainties in Table I aligns well with the PDF uncertainties of Fig. 5. In particular, the MSTW2008NLO strange-quark error band is much narrower than that of the other sets because of the implicit assumption in the MSTW global fit that all sea quarks have the same universal $q_i(x, Q_0^2) \sim x^\delta$ behaviour as $x \rightarrow 0$. In practice, the parameter δ is determined quite precisely by the fit to the HERA small- x structure function data.

Of the two ratios, R_c^\pm is less affected by the choice of selection cuts. Modifying the lepton and jet cuts, within experimentally reasonable ranges, changes R_c^\pm by only a few percent. R_c is more sensitive to the selection cuts with the value changing by up to $\mathcal{O}(30\%)$.

When in future more high-statistics data are available, the ratios R_c^\pm and R_c can also be considered as distributions of kinematic observables, e.g. the W transverse momentum as shown at LO (using NLO PDFs) in Fig. 6 for R_c^\pm . In contrast to R^\pm , which is related to the u/d ratio at high x and therefore *increases* with p_T^W , R_c^\pm is a *decreasing* function of p_T^W driven by the dominance of the valence d -quark at high x over the other parton distri-

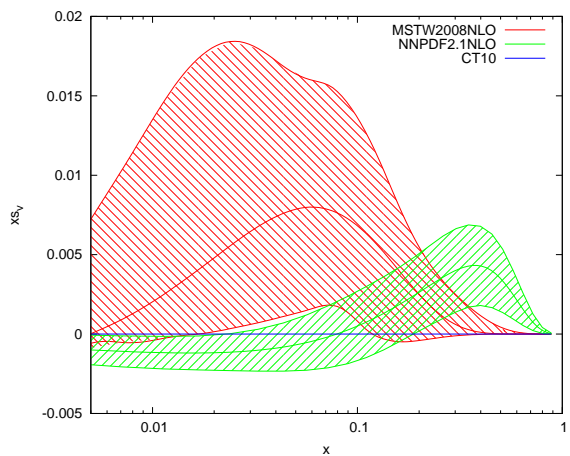


FIG. 4: Strange valence distribution for NLO PDFs at $Q = M_W$. For MSTW2008NLO and NNPDF2.1, the shaded bands correspond to the 68%cl PDF uncertainty.

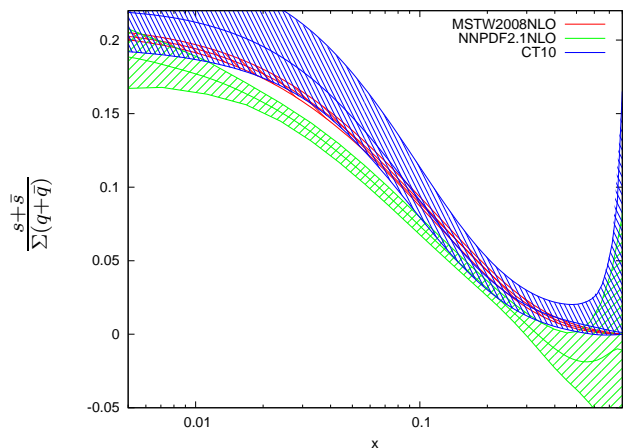


FIG. 5: NLO PDF ratio of $s + \bar{s}$ to $\Sigma(q + \bar{q})$ at $Q = M_W$.

butions involved, see (5). This decrease of R_c^\pm is obtained for all PDF sets but the rapid drop for NNPDF is a result of both \bar{d}/d at large x and also the increasing value of s_v at large x as shown in Fig. 4. Similar conclusions can be drawn by considering R_c^\pm as a function of the W rapidity as shown in Fig. 7.

III. PREDICTIONS FOR $\sigma(Z + c)$

Even though the corresponding cross sections with the W boson replaced by a Z boson are significantly smaller, especially when account is taken of the difference in leptonic branching ratios, with a sufficiently large data sample a similar analysis can be performed.

We first consider the ratio

$$R_c^Z = \frac{\sigma(Z + c)}{\sigma(Z + \text{jet})}, \quad (7)$$

where the c in the numerator here refers to either a c or a

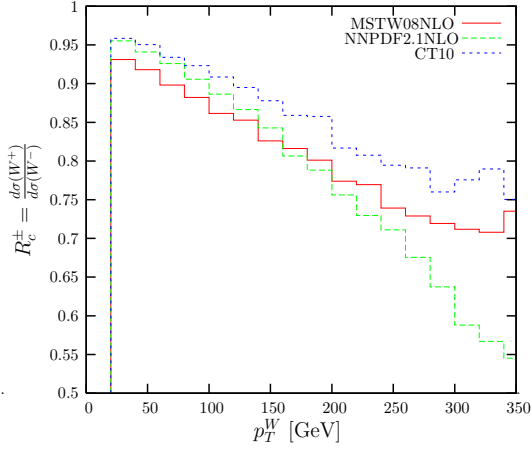


FIG. 6: Dependence of R_c^\pm on p_T^W using NLO PDFs.

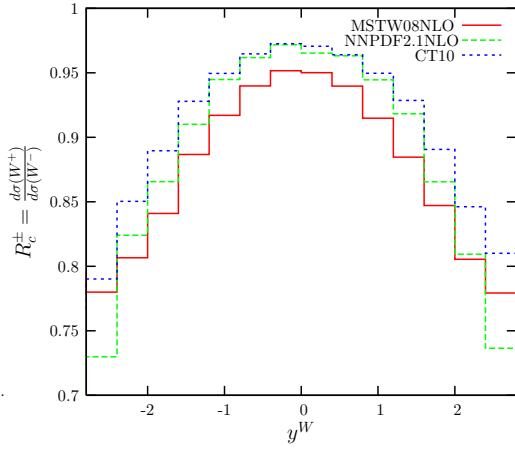


FIG. 7: Dependence of R_c^\pm on y^W using NLO PDFs.

\bar{c} jet. Defining a similar set of experimental cuts: $p_T^j > 20$ GeV, $|\eta^j| < 2.1$, $p_T^l > 25$ GeV, $|\eta^l| < 2.1$, $R = 0.5$, $R^{lj} = 0.3$ and $60 < m_{ll} < 120$ GeV, gives the NLO ratio predictions shown in Table IV, now with the QCD scales set to M_Z . (Note that MCFM also includes the photon (γ^*) contribution to the Z +jet cross sections, consistent with the experimental analysis, but the number of photon events is strongly suppressed by the cut on the lepton pair invariant mass.)

PDF set	R_c^Z
CT10	$0.0619^{+0.0032}_{-0.0032}$
MSTW2008NLO	$0.0640^{+0.0014}_{-0.0016}$
NNPDF2.1NLO	0.0660 ± 0.0013
GJR08	0.0611 ± 0.0011
ABKM09	0.0605 ± 0.0019

TABLE IV: Comparison of R_c^Z NLO predictions for the different PDF sets, with 68%cl PDF uncertainties.

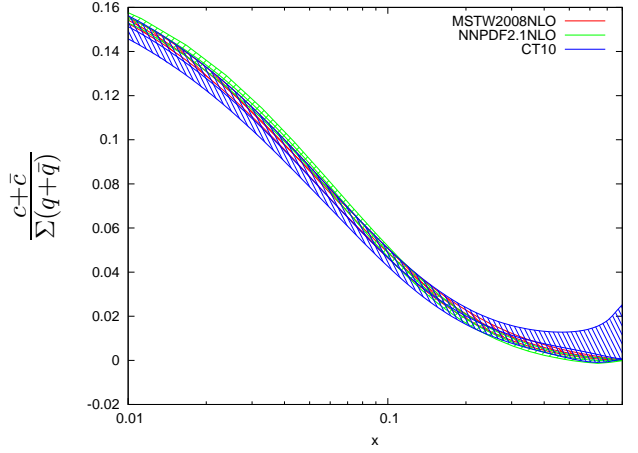


FIG. 8: Charm quark fraction $(c + \bar{c})/\Sigma(q + \bar{q})$ at $Q = M_Z$ for NLO PDFs.

In principle R_c^Z provides direct information on the charm content of the proton, complementary to that obtained from DIS experiments via F_2^c .

We note that the differences between the predictions of different PDF sets are much smaller than for the strange quark distributions, presumably because in all these global fits the charm distributions arise perturbatively from $g \rightarrow c\bar{c}$ splitting, with the small- x gluon well determined from the HERA structure function data. This can be seen in Fig. 8, which compares the ratio of charm quarks to all quarks for the three PDF sets. When PDF errors are taken into account the three sets are very difficult to distinguish, and this is reflected in the similarity in the R_c^Z predictions in Table IV. The use of R_c as a PDF discriminator will therefore require a very precise measurement.

We can also consider the (charm) charge asymmetry ratio:

$$R_c^\pm(Z) = \frac{\sigma(Z + \bar{c})}{\sigma(Z + c)}. \quad (8)$$

At first sight it might appear that $R_c^\pm(Z)$ is automatically equal to 1, but this is only true if $c = \bar{c}$ in the initial state. This is indeed the case for all the PDF sets considered here, since as already noted the charm distributions are generated by charge symmetric $g \rightarrow c\bar{c}$ splitting. However this symmetry does not necessarily hold if we allow for an *intrinsic* charm component [13]. PDF studies incorporating intrinsic charm, see for example [7, 14], suggest that it is probably a small effect compared to perturbatively generated charm, particularly at the small x values relevant to the LHC. In any case, any such intrinsic charm analysis is highly model dependent, and beyond the scope of the present study. We do note however that in the process $qg \rightarrow Zq$, which dominates Z +jet production over most of the kinematic range at the LHC, the ‘ q ’ is more likely to be positively charged than negatively charged, and the q -jet is therefore more likely to contain a μ^+ (say) than a μ^- . Hence there may

well be a ‘natural’ charge asymmetry in the misidentified charm-jet background.

Finally we can also compare the ratios:

$$R_c^{WZ} = \frac{\sigma(Z+c)}{\sigma(W+c)} \quad \text{and} \quad R^{WZ} = \frac{\sigma(Z+\text{jet})}{\sigma(W+\text{jet})}. \quad (9)$$

The NLO predictions for MSTW2008NLO are 0.045 and 0.082 respectively, for the selection cuts described above for W and Z including leptonic decays. We can relate the ratio of these ratios to the ratio of $s + \bar{s}$ over $c + \bar{c}$ which can be read from Figs. 5 and 8 at the appropriate momentum fraction. Of course in practice it is more complicated, as multiple scales, momentum fractions and couplings are involved, but an estimate $R^{WZ}/R_c^{WZ} \sim 2$ can be extracted for this ratio and this matches well with the 0.082/0.045 ratio above.

IV. CONCLUSIONS

We have investigated charm production in association with W and Z bosons at the LHC. We have presented predictions relevant to the recent (and ongoing) CMS analysis for W bosons produced in association with a charm-quark jet. Use of a larger LHC data sample should lead to precise measurements of the ratios R_c and R_c^\pm which can in turn provide useful information on the

strange content of the proton, and in particular the asymmetry between s and \bar{s} at small x and high Q^2 . We have also shown results for several differential distributions that can in principle be used to provide additional information on the x dependence of the strange and anti-strange quark distributions. We also propose a measurement of the corresponding ratio for Z bosons, R_c^Z , which can be used as a measure of the charm content of the proton.

Finally, we note that information on the strange quark content of the proton can also be obtained by comparing the *total* W and Z cross sections at the LHC, see for example the recent ATLAS study reported in [15]. This exploits the fact that the dependence on the strange PDF is linear for the W and quadratic for the Z : $\sigma(W) \sim c\bar{s} + \bar{c}s + \dots$, $\sigma(Z) \sim s\bar{s} + \dots$. The method is complementary to the charm-jet tagging method discussed in the present study, and it will be interesting to compare the results from the two analyses when more precise data become available.

Acknowledgements

Useful discussions with Isabel Josa and Robert Thorne are acknowledged. EV is grateful to the UK Science and Technology Facilities Council for financial support.

-
- [1] H. L. Lai, P. M. Nadolsky, J. Pumplin, D. Stump, W. K. Tung and C. P. Yuan, JHEP **0704** (2007) 089 [arXiv:hep-ph/0702268].
 - [2] T. Aaltonen *et al.* [CDF Collaboration], Phys. Rev. Lett. **100**, 091803 (2008) [arXiv:0711.2901 [hep-ex]].
 - [3] V. M. Abazov *et al.* [D0 Collaboration], Phys. Lett. B **666**, 23 (2008) [arXiv:0803.2259 [hep-ex]].
 - [4] CMS Collaboration, CMS-PAS-EWK-11-013.
 - [5] J. M. Campbell and R. K. Ellis, <http://mcfm.fnal.gov/>.
 - [6] H. L. Lai, M. Guzzi, J. Huston, Z. Li, P. M. Nadolsky, J. Pumplin and C. P. Yuan, Phys. Rev. D **82**, 074024 (2010) [arXiv:1007.2241 [hep-ph]].
 - [7] A. D. Martin, W. J. Stirling, R. S. Thorne and G. Watt, Eur. Phys. J. C **63**, 189 (2009) [arXiv:0901.0002 [hep-ph]].
 - [8] R. D. Ball *et al.* [The NNPDF Collaboration], Nucl. Phys. B **855**, 153 (2012) [arXiv:1107.2652 [hep-ph]].
 - [9] M. Gluck, P. Jimenez-Delgado and E. Reya, Eur. Phys. J. C **53**, 355 (2008) [arXiv:0709.0614 [hep-ph]].
 - [10] S. Alekhin, J. Blumlein, S. Klein and S. Moch, Phys. Rev. D **81**, 014032 (2010) [arXiv:0908.2766 [hep-ph]].
 - [11] <http://hepforge.cedar.ac.uk/lhapdf/>
 - [12] M. Goncharov *et al.* [NuTeV Collaboration], Phys. Rev. D **64** (2001) 112006 [arXiv:hep-ex/0102049].
 - [13] S. J. Brodsky, P. Hoyer, C. Peterson and N. Sakai, Phys. Lett. B **93** (1980) 451.
 - [14] J. Pumplin, H. L. Lai and W. K. Tung, Phys. Rev. D **75** (2007) 054029 [arXiv:hep-ph/0701220].
 - [15] G. Aad *et al.* [ATLAS Collaboration], arXiv:1203.4051 [hep-ex].